Optimizing Mixtures of Alkali Aluminosilicate Cement Based on Ternary By-Products

Hoang Vinh Long [1*]

[1] *Faculty of Building Materials, National University of Civil Engineering, Hanoi, Vietnam.*

Abstract

Portland cement is a popular binder but causes many adverse effects on the environment. That is due to the large consumption of raw materials and energy during production while emitting vast amounts of CO_2. In recent years, Alkali Aluminosilicate Cement (AAC) has drawn much attention in research and development and promises to become a binder that can replace the traditional cement. In many studies of this binder, the content of the ingredients is often gradually changed to determine the optimal composition. The object of this paper is to optimize the composition of AAC using a combination of three by-products as the primary raw material, including Rush Husk Ash (RHA), Fly Ash (FA), and Ground Granulated Blast-Furnace Slag (GGBS). The investigation was conducted based on the critical parameter SiO_2/Al_2O_3, and the D-optimal design. The FA and the GGBS were industrial product form, while the RHA was ground in a ball mill for 2 hours before mixing. The results show that this type of binder has setting time and soundness to meet standard cement requirements. While comparing to Portland cement, the AAC has a faster setting time, slower development of compressive strength in the early stages but a higher strength at the age of 56 days. According to the highest compressive strength at 28 days and high fly ash content, the optimal composition was RHA of 27.8%, FA of 41.8%, and GGBS of 15.4%, corresponding to the ratio SiO_2/Al_2O_3 of 3.83. In addition, compressive strength at 28 days of the mortar specimens with the optimal binder and the ratio of water/ cement at 0.32 reached 63 MPa.

Keywords: Alkali Aluminosilicate Cement; Rice Husk Ash, Fly Ash, Ground Granulated Blast- Furnace Slag, D-Optimal Design.

1. Introduction

"Geopolymer" is a term commonly used to refer to a binder that is synthesized from two-part consisting of solid aluminosilicate materials and alkaline activators [1, 2]. With such structural formation, the binder can also be known by other different names, such as alkali-activated cement, alkali alumosilicate cement, etc. Gluskhovsky [3] is believed to be the pioneer to examine the binder used in some constructions in the ancient Roman and Egyptian periods. He suggested that these works were made up of an aluminosilicate calcium hydrates compound similar to Portland cement and crystalline phases of analcite. In the past few decades, many studies have focused on using solid wastes to make alkali-activated concrete such as blast furnace slag, metakaolin, coal fly ash, red mud, etc. [4, 5]. That could be a promising solution to recycling waste sources into sustainable materials, contributing to environmental protection. Compared with Portland cement, AAC offers some significant benefits such as lower CO_2 emissions (up to 80%) [6], 43% less energy consumption, and uses of 25% less water [7].

Vietnam is a developing country with abundant sources of industrial and agricultural wastes, in which FA, rice husks, and blast furnaces slag are most notable. FA is a by-product of thermal power plants. Currently, Vietnam has 25 coal-fired power plants that emit a total amount of ashes of more than 19.5 million tons/ year, in which FA accounts for about 80-85%. The amount of ash consumption has been only about 38% of the total emissions [8]. FA has a round fine granular form and contains mainly glassy phase, so it has a high activity often used in concretes. Paddy production achieves more than 40 million tons in Vietnam each year on average. The volume of rice husks accounts for 20% of the composition of paddy, so each year, approximately 9 million tons of rice husks are discharged into the environment. That is a tremendous amount of waste; otherwise, the disposal will pollute the environment and be a prodigal raw material. A suitable burning regime can make RHA with amorphous and highly active silica content from rice husk, even producing ultra-high performance concrete [9, 10]. Blast furnace slag is a by-product of the iron and steel industry. In Vietnam, a large slag volume is generated annually at 4.23 million tons in 2018 and 7.1 million tons in 2020 [11]. GGBS is mainly a glassy phase, has a high calcium oxide content, and can hydrate to enhance the strength and durability of concrete.

AAC can be divided into three main groups: calcium-rich binders, low-calcium binders, and hybrid binders [4]. To make the third one, it is usually a combination of alumosilicate precursors and calcium-rich materials such as portland cement clinker, GGBS. Due to colossal emission and environmental impact, class-F FA is of significant interest to research and use as an alumosilicate prime material to produce AAC. Numerous studies have reported that the base-FA alkaline-activated binders have a long setting time. In order to stimulate reactions, it is often necessary to use high alkaline content or elevated temperature of 60- 200ºC [4]. GGBS is used in combination with FA to create mutual effects such as increasing workability, ensuring setting time, and increasing strength [12]. RHA has also been studied in combination with FA to provide SiO_2 and increase the setting time [13]. RHA is usually added to the alkaline-activated binders in two forms: powder form mixed with other raw materials [14, 15] or combined with NaOH to make liquid glass [16, 17].

The properties of AAC are commonly dependent on many factors, especially on activators and prime materials' chemical composition and content. Ratio SiO_2/Al_2O_3 is considered an important parameter influencing the properties of this binder [18, 19]. In numerously previous studies, the content of materials changes progressively to investigate influential factors and figure out the optimal mix of two components probably [20]. The simplex centroid design method was used with seven mixes to determine the regression function and the optimal component in some research [21]. D-optimal experimental design is an effective method to optimize the ingredients and is usually applied to three components [22].

This paper focuses on using the D- optimal method to determine the optimal combination of RHA, FA, and GGBS to produce AAC. The variation range of the raw components is selected based on SiO_2/Al_2O_3 ratio. The results could contribute to the more practical application of industrial and agricultural wastes towards sustainable development.

2. Materials and Methods

2.1. Materials

Rice Husk Ash (RHA)

RHA burned in a Torbed industrial incinerator was used in this study. The Torbed incinerator has a cycle of burning rice husk with a temperature of 820-830ºC, so the amount of active SiO_2 is quite large, and the LOI content is low. A 5- liter ball mill was used to grind the RHA for 2 hours. Some of the physical properties of RHA are given in Table 1, and the chemical compositions are shown in Table 4. The RHA contains mainly SiO_2 with a content of 87.21%, the loss on ignition was 5.87%, and a negligible amount of other oxides.

Table 1. Physical properties of the RHA

Properties	Unit	Results
Specific gravity	g/cm³	2.14
Strength activity index, %	%	109
Mean particle size	μm	6.95
Average pore diameter	Nm	9.64
Specific surface area (BET)	m²/g	143.5

Fly ash (FA) and Ground- Granulated Blast- Furnace Slag (GGBS)

A class F fly ash provided by Pha Lai thermal power plant was used as an alumosilicate precursor. GGBS was an industrial product obtained from Hoa Phat Hai Duong steel company. The FA and GGBS's physical properties and

chemical compositions are presented in Tables 2 and 4, respectively. The FA has a total of SiO_2, Al_2O_3, and Fe_2O_3 content of 87.44% and CaO of 1.17%. GGBS has the basicity coefficient CaO+ MgO/ SiO_2+ Al_2O_3 was 0.95.

Table 2. Physical properties of the FA and GGBS

Properties	FA	GGBS
Specific gravity, g/cm^3	2.21	2.89
Strength activity index at the age of:		
7 days	-	82.5
28 days	86.04	103.2
Average particle size, μm	18.79	
Specific surface area (Blaine)	-	5200

Cement

The PC40 cement from But Son cement factory has the physical properties that meet Type-I cement requirements of ASTM C150-20 [23]. The PC40 cement was used as a control sample against the AAC. Tables 3 and 4 show the physical properties and the chemical compositions of the PC40 cement, respectively.

**Table 3. Physical properties of the PC40 cement**

Properties	Unit	Result
Specific gravity	g/cm^3	3.1
Fineness		
- Retained 0.09 mm	%	2.1
- Average particle size	μm	16.64
Normal Consistency	%	30.5
Soundness	mm	1.15
Time of setting; Vicat test		
- Initial setting time	minutes	130
- Final setting time	minutes	210
Compressive strength		
- 3 days	MPa	30.75
- 28 days	Mpa	44.42

Table 4. Chemical compositions of the RHA, FA, GGBS, and PC40 cement (%)

	SiO_2	Al_2O_3	CaO	MgO	MnO	K_2O	Na_2O	Fe_2O_3	SO_3	TiO_2	LOI
RHA	87.21	0.42	0.94	0.43	-	1.76	0.57	1.60	-	-	5.78
FA	54.01	27.90	1.17	1.48	-	4.44	-	5.53	-	-	4.64
GGBS	34.58	13.98	36.45	9.45	1.63	1.32	0.28	0.53	0.50	0.65	0.46
PC40 Cement	21.94	5.16	63.70	2.04	-	0.72	0.13	3.29	1.01	0.06	1.47

A Horiba laser LA-950 analyzed the particle distribution of the prime materials shown in Figure 1. The median particle sizes of RHA, FA, GGBS, and PC40 cement were 7.09, 18.79, 9.53, and 16.64 μm, respectively. Thus, the particle size of the alumosilicate mixture is equivalent to that of PC40 cement.

At the same time, in this study, some alkaline activators consisting of sodium hydroxide (NaOH), sodium carbonate (Na_2CO_3), liquid glass (Na_2SiO_3), and calcium oxide (CaO) were used. The water glass had solution modulus M_s of 3, and other activators are anhydrous with purity up to 99%. Tartaric acid ($C_4H_6O_6$) with powder form was used as a retarder. Graded standard sand was fine aggregate for casting the mortar specimens. Superplasticizer Sikament R4 was used to adjust the flow of mortar.
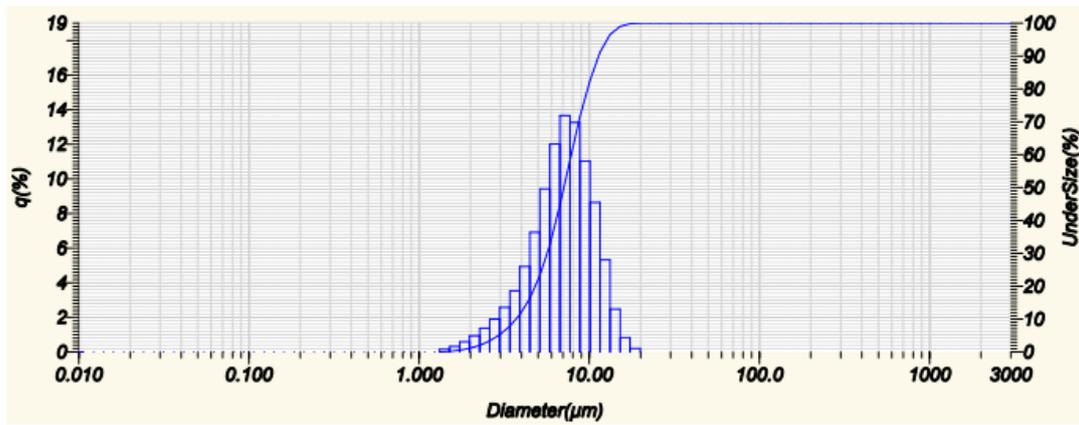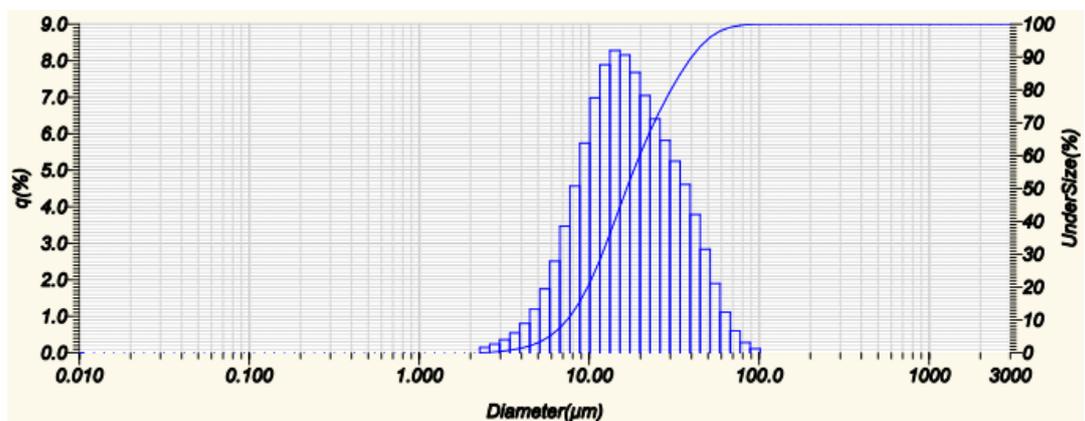
(a) Rice husk ash
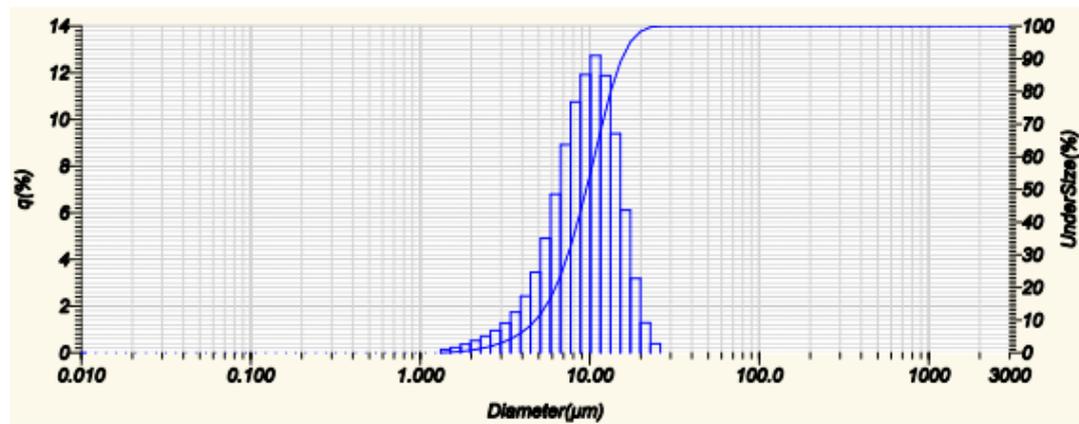
(b) Fly ash
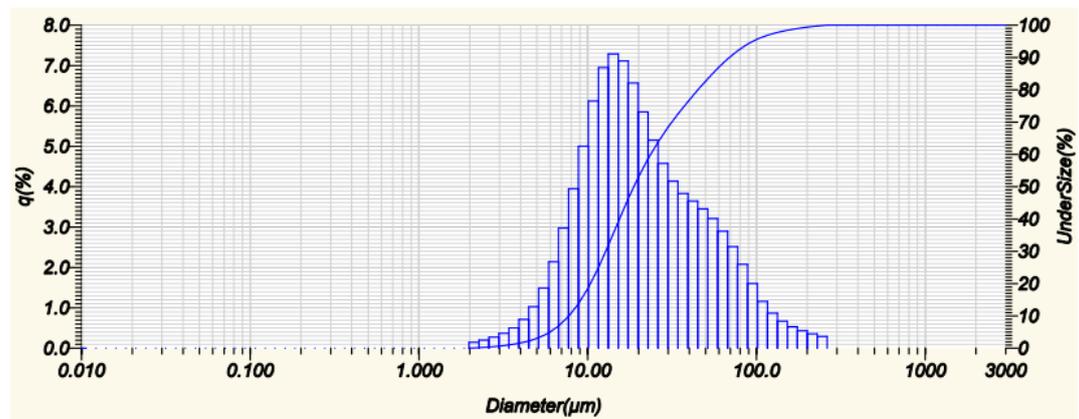
(c) Ground granulated blast- furnace slag

(d) PC 40 cement

Figure 1. Particle distribution of the RHA, FA, GGBS, and PC40 cement

2.1. Methods

A Vicat needle apparatus was used to measure normal consistency and setting times according to ISO 9597: 2008 [24]. The mortar samples were used to evaluate the strength development that was prepared according to the following procedure: First, a paste mixture comprised a binder, and water was mixed in an Ele mixer at a slow speed of 62± 5 RPM for the 30 s, then followed by the addition of sand with binder/ sand ratio of 1:3 and another 30 s of mixing. Next, the mixer worked at high speed of 125±10 RPM for an additional 30 s. Stop the machine for 30 s, use a rubber or plastic trowel to scrape the mortar stick to the wall and the bottom of the mixer's bowl and apply it to the center of the bowl. After that, continue mixing at high speed for an additional 60 s. The fresh mortar mixture was cast into molds with dimensions of 40×40×160 mm. The specimens were plastic cover-cured inside molds in ambient conditions for 24 hours. Then, they were de-molded and kept in submerged water until conducting tests at ages of 3, 7, 28, and 56 days. The compressive and flexural strength of mortar samples were determined according to ISO 679: 2009 [25].

Figure 2. Mortar specimens and the equipment for measuring compressive strength and flexural strength

At the age of 28 days, mortar specimens were prepared to capture microstructure with JEOL JSM-7600F field-emission SEM Scanning electron microscope.

The procedure of optimizing AAC

The variation ranges of three materials consisting of RHA, FA, and GGBS were calculated based on the reasonable SiO_2/Al_2O_3 ratio suggested in previous studies. Then D-optimal design and Design Expert 7.0 software was used to determine an experimental plan. After that, the paste and mortar specimens were cast following the experimental plan and were evaluated properties. Based on Design-Expert 7.0 software, two regression functions for compressive strength of mortar samples at 28 days and 56 days were figured out. As a result, the factors affecting the compressive strength of the mortar sample can be assessed, and the optimal compositions of AAC were selected.

3. Results and Discussion

3.1. An Experimental Plan

In this study, the total amount of the additives was fixed at 15% by weight with the ratio of NaOH: Na_2CO_3: Na_2SiO_3: CaO: acid Tartaric was 4.5: 3: 3: 4: 0.5 (%). The total content of RHA, FA, and GGBS was 85% by weight. Commonly, an alkali-activated binder has the ratio SiO_2/Al_2O_3 of 4 [26]. Besides, Palomo et al. [27] reported that the ratio of SiO_2/Al_2O_3 doubled in the case when using liquid glass and NaOH as the activator, compared to the case of using NaOH only. Based on that, the range of content variation was selected as 25% $\leq$RHA$\leq$ 35%, 30%$\leq$FA$\leq$ 45%, and 15%$\leq$GBBS$\leq$30% and denoted RHA as A, FA as B and GBBS as C. Correspondingly, the ratio of SiO_2/Al_2O_3 of the raw material mixture is in range of 3.56- 4.85. A D-optimal design with 16 AAC mixes was used to set up an experimental plan. There are 11 different proportions of binder components and five proportions to calculate the iteration accuracy. The composition of the cement mixture in the experimental plan is given in Table 5.

3.2. Properties of the AAC

The properties of the mixture of AAC are shown in Tables 5 and Figure 3. The normal consistency of the binders in the range 18-21% is much lower than that of the PC40 cement at 30.5%. That could account for the ball bearing effect of fly ash due to spherical-shaped particles of this material. Besides, GGBS also contributes to decreasing the viscosity of cement pastes [28].

Figure 3 shows that in cases of the AAC, the initial time of setting was in the range of 55-103 minutes and higher than 45 minutes. Besides, the final time of setting was in the range of 105-166 minutes and less than 375 minutes. Therefore, both setting times of the binder satisfy the requirement of TCVN 2682: 2009 [29], conforming to general construction applications of concrete. However, the setting times of the binder was relatively short compared to that of PC40 cement at 130 minutes and 210 minutes, respectively. It is agreed with P. Nath and P. K. Sarker's report that GGBS reduces the setting time of alkaline-activated binder [12]. The soundness of the AAC was in the range 0.97-2.47 mm, moderately less than 10 mm as a requirement of TCVN 2682: 2009 [29]. The soundness is approximately equivalent to that of the control cement sample with 1.15 mm.

Table 5. Compositions and properties of the AAC

| Mix no.	RHA	FA	GGBS	Normal consistency (%)	Setting time (min)		Soundness (mm)
					Initial	Final	
1	25	37.5	22.5	19.0	68	128	1.23
2	30	40	15	19.0	93	145	1.5
3	30	35	20	20.0	65	120	1.53
4	30	30	25	20.0	80	156	1.5
5	30	32.5	22.5	20.0	86	150	1.10
6	25	30	30	19.0	55	106	1.87
7	35	35	15	20.5	103	166	1.47
8	35	30	20	21.0	65	125	0.97
9	35	35	15	20.5	76	138	2.13
10	25	37.5	22.5	19.0	62	105	1.43
11	27.5	40	17.5	18.5	68	105	1.90
12	25	45	15	18.0	94	155	2.20
13	25	45	15	18.0	80	110	2.47
14	25	30	30	19.0	72	120	1.67
15	35	32.5	17.5	21.0	65	120	1.83
16	35	30	20	21.0	81	150	1.47
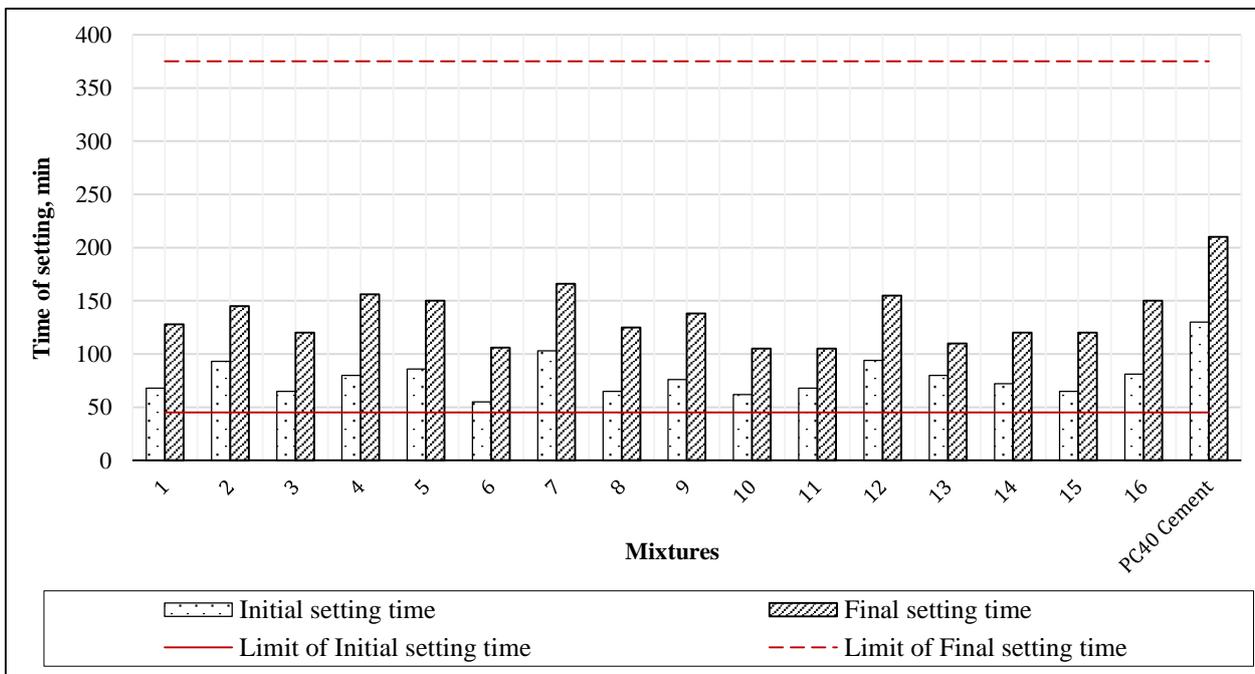
Figure 3. Time of setting of AAC and PC40 cement

3.3. Properties of Mortars based on the AAC

The mortar samples were prepared with a water to cement ratio of 0.32, cement to the sand ratio of 1: 3, and the binder compositions presented in Table 5. The superplasticizer R4 to the cement ratio was fixed at 1.35% to ensure the

flow of fresh mortar at 110±5%. The control mortar specimens using PC40 cement with the same water to cement ratio and R4 to cement ratio also were cast. Both compressive and flexural strength of mortar specimens were measured at ages of 3, 7, 28, and 56 days and given in Table 6.

3.4. Properties of Mortars based on the AAC

The mortar samples were prepared with a water to cement ratio of 0.32, cement to the sand ratio of 1: 3, and the binder compositions presented in Table 5. The superplasticizer R4 to the cement ratio was fixed at 1.35% to ensure the flow of fresh mortar at 110±5%. The control mortar specimens using PC40 cement with the same water to cement ratio and R4 to cement ratio also were cast. Both compressive and flexural strength of mortar specimens were measured at ages of 3, 7, 28, and 56 days and given in Table 6.

Table 6. Compressive strength and flexural strength of mortar specimens

| Mix No.	Compressive strength (MPa)				Flexural strength (MPa)			
	3 days	7 days	28 days	56 days	3 days	7 days	28 days	56 days
1	13.41	24.89	40.44	40.57	2.56	4.80	5.78	5.62
2	16.42	35.93	49.29	53.08	1.60	4.16	5.47	8.33
3	13.46	24.67	38.98	35.85	0.73	3.27	3.56	5.64
4	13.25	24.74	40.66	41.01	2.44	4.75	6.56	6.80
5	13.71	25.08	40.76	45.93	2.24	4.52	5.63	5.68
6	18.93	31.81	46.34	52.14	0.88	4.48	4.55	6.76
7	7.84	17.77	34.00	34.48	1.55	4.20	4.92	5.37
8	14.86	26.09	41.98	42.30	2.63	4.95	6.02	4.22
9	7.52	17.94	33.78	35.32	1.38	4.31	5.31	5.44
10	11.49	20.08	36.03	37.30	2.23	4.32	5.39	5.60
11	19.18	38.69	52.41	60.90	1.39	4.99	8.64	9.52
12	7.02	18.44	45.33	47.99	1.67	4.49	6.33	6.29
13	20.64	33.03	45.38	46.56	1.77	4.48	6.33	6.21
14	17.60	31.71	47.39	51.59	1.48	4.44	5.31	6.03
15	8.88	18.62	34.84	33.09	0.93	3.55	4.14	4.90
16	14.80	25.85	42.81	47.84	2.16	4.64	6.02	6.13
Control	44.92	61.81	66.84	68.23	5.45	5.70	10.51	10.62
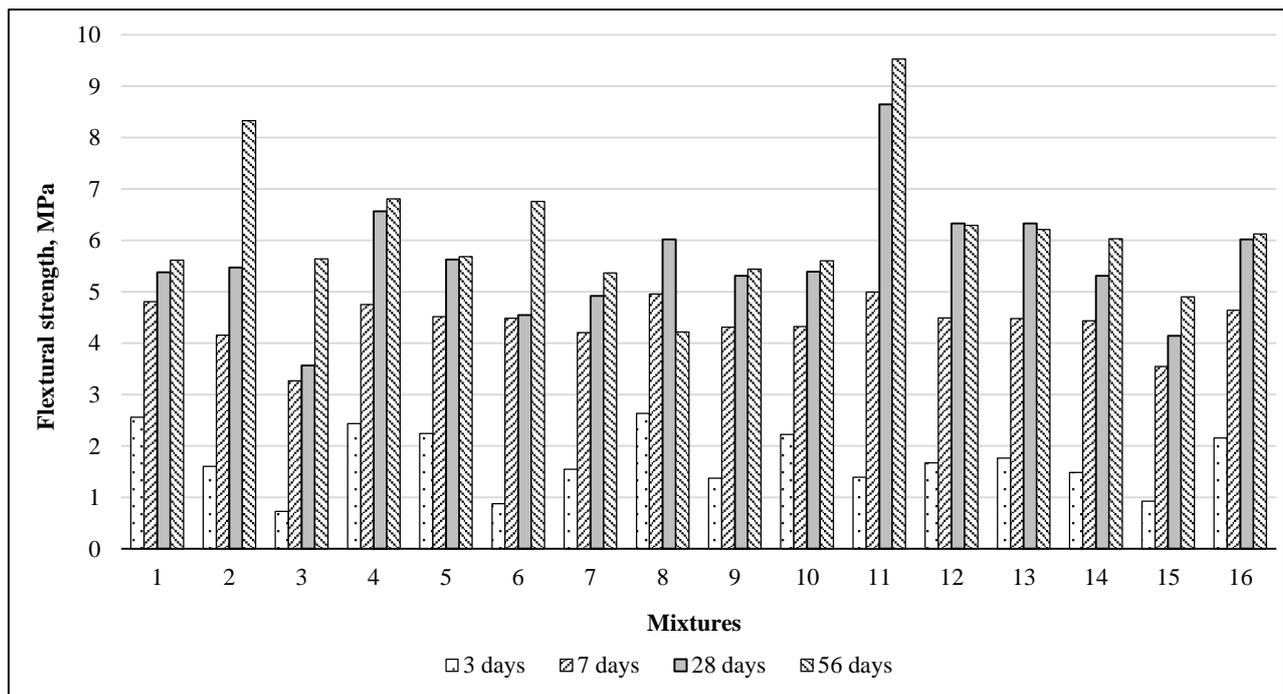
Figure 4. Development of flexural strength of mortar specimens

Flexural strength of mortar samples using AAC were in the range of 3.56-8.94 MPa and 4.22- 9.52 MPa at 28 days and 56 days, respectively. Those are relatively lower than that of Portland cement samples at 10.51 and 10.62 MPa, respectively. The ratio of flexural strength to compressive strength at 28 days average was 1: 7.5, against the Portland cement sample at 1: 6.4.
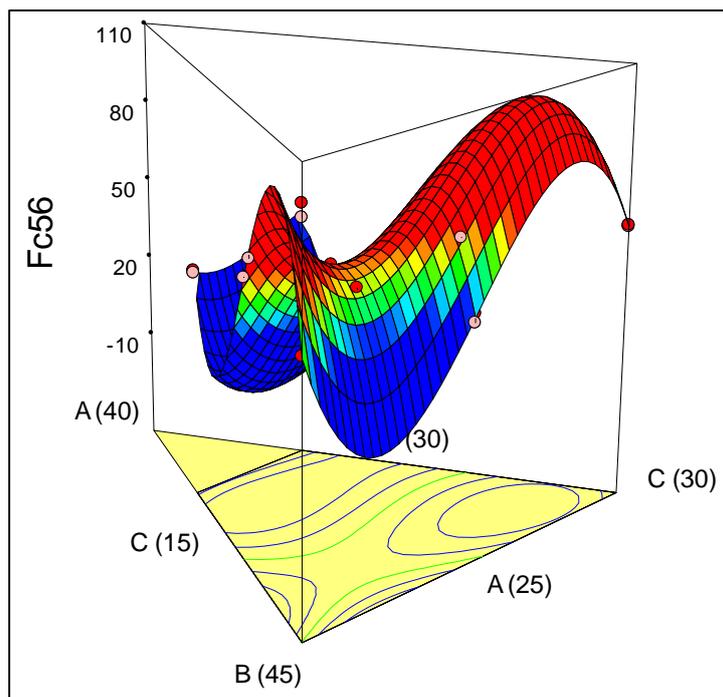
Two regression functions of the mortar compressive strength at 28 days and 56 days were figured out by Design Expert 7.0 software as follows:

$f'_{c28}= 236.26A+ 45.33B+ 46.85C - 446.43AB-450.10AC -31.27BC +870.25ABC- 536.00AB(A-B)- 416.93AC(A-C) - 95.67BC(B-C)$

$f'_{c56}=631.65A+47.23B+51.82C-1329.52AB-1344.12AC-42.04BC +2518.14ABC-1442.72AB(A-B) -1282.36AC(A-C) -387.90BC(B-C)$
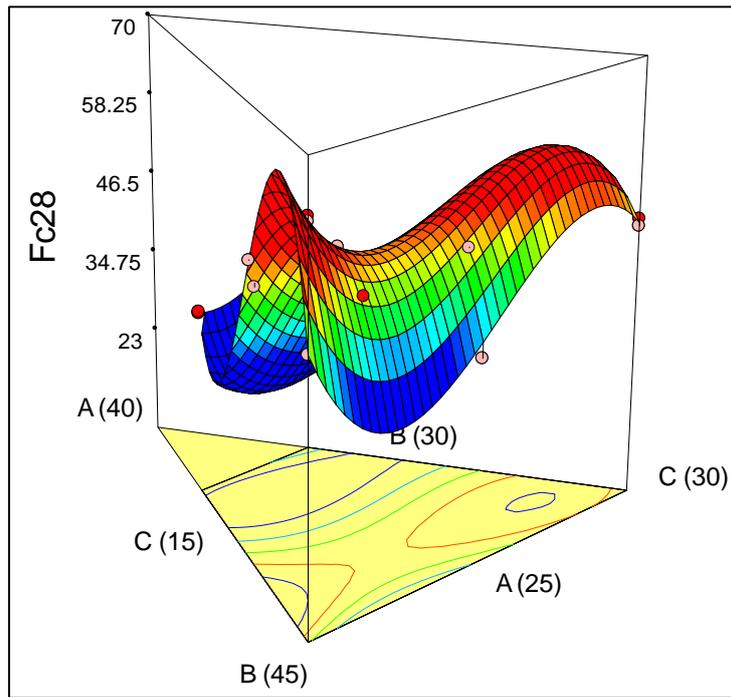
(a) 28 days

(b) 56 days

Figure 5. Response surface of compressive strength at the age of (a) 28 days; and (b) 56 days

The Model F-value of 26.31 and 23.81 implies, respectively, that the models f'$_{c28}$ and f'$_{c56}$ are significant. At the same time, the "Lack of Fit F-value" of 0.39 and 0.85 implies the Lack of Fit of the two models is not significant, meaning the pure error. The response surfaces of the two regression functions are shown in Figure 5.

Comparing Figures 5 (a, and b) shows that the highest compressive strength area is shifted towards higher GGBS content at about 25%. The shift indicates that GGBS enhances the long-term strength of the mortar sample using the AAC. It may be due to the long-term hydration of GGBS contributing to strength development [30]. With the highest compressive strength criteria at the age of 28 days and significant FA content, the optimal mixture with the binder content was RHA of 27.78%, FA of 41.84%, and GGBS of 15.38%, corresponding to the ratio SiO_2/Al_2O_3 of 3.83. Figure 6 (b) shows that the pick of compressive strength at 28 days is related to the ratio SiO_2/Al_2O_3 in the range of 3.8-3.9. Simultaneously, the optimal mixture with the highest compressive strength was RHA of 27.0%, FA of 32.4%, and GBBS of 25.6%, with the ratio of SiO_2/Al_2O_3 of 4.01.

For comparison, two group samples were cast with the first optimal mixture and a control sample with PC40 cement at the same cement to the sand ratio and the water to cement ratio. The strength development of the two-group samples is shown in Figure 6(a). The compressive strength of the samples using the optimal cement at 3, 7, and 28 days of age achieved 14.31, 46.91, and 63.52 MPa, respectively. These values are all lower than those with Portland cement at 44.92, 61.81, and 66.84 MPa, respectively. As a result, the development of compressive strength of the mortar using the AAC is slower than that of the Portland cement specimen in the early stages. However, the result of the setting time shows that ACC can have a faster reaction rate in a very early stage. Contrary, the compressive strength of the former at 78.96 MPa was 16% higher than that of the latter at 68.23 MPa at 56 days. Darsanasiri et al. [15] reported that the compressive strength of AAC mortar with RHA of 30%, FA of 35%, and GGBS of 20% was always higher than that of Type-I portland cement. However, they used a class-C FA with calcium oxide of 22.2% in their investigation. That probably causes faster strength development. Besides, compressive strength at 28 days and 56 days was 63.52 MPa and 78.96 MPa in the experiment, compared with that calculated through the regression functions of 61.42 and 83.92, respectively. The difference is not significant.
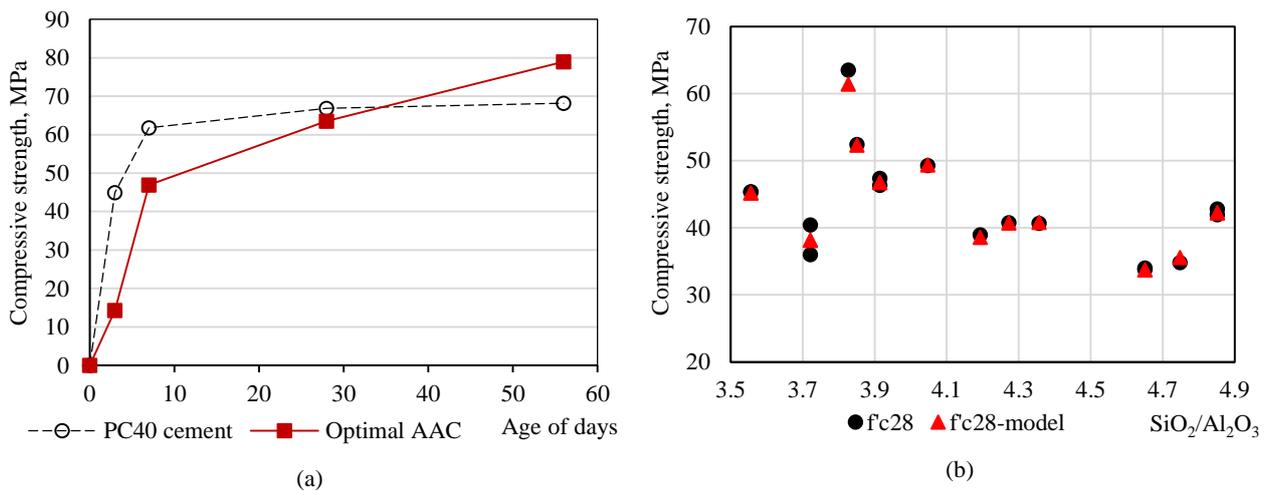

| (a) | (b) |

Figure 6. The comparison of mortar compressive strength (a) with the optimal AAC and the PC40 cement; (b) At 28 days in the experiment (f'c28) and the model (f'c28-model)
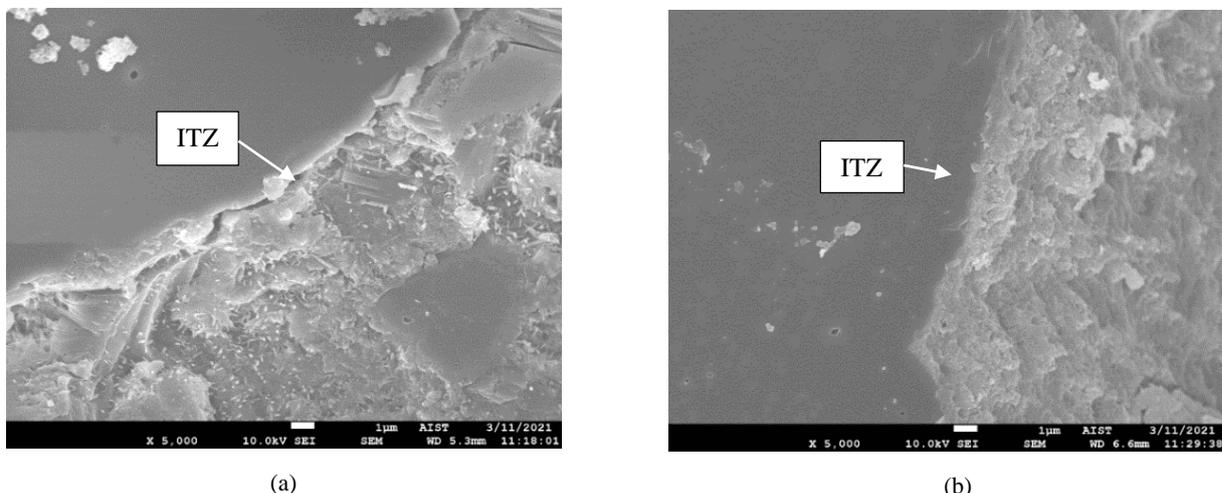

| (a) | (b) |

Figure 7. SEM images of the interfacial transition zone (ITZ) of mortar specimens: (a) PC40 cement; (b) AAC

Figure 7 shows a microstructure image of mortar specimens with Portland cement and the AAC at 28 days. It can be seen the "spikes" of the mineral CSH in Figure 7(a). Moreover, the bond between the aggregate surface and the AAC is close, and reaction products seem to form dense structures in Figure 7(b).

4. Conclusions

The test results proved that it is possible to develop sustainable cement from agricultural and industrial by-products as primary raw materials, including RHA, FA, and GGBS. Based on the data generated in this experimental work, the following conclusions can be drawn:

- The AAC has a smaller normal consistency, shorter setting time, and equivalent soundness than those of the Portland cement; however, all meet TCVN 2682: 2009 specifications.

- Mortar specimens using the AAC with the ratio of water/ cement at 0.32 and the ratio of R4/ cement at 1.35% had a flow rate of 110± 5% and reached compressive strength at 28 days of 63 MPa.

- The optimal composition of the alkali alumosilicate cement was RHA of 27.8%, FA of 41.8%, and GGBS of 15.4%, with the ratio SiO_2/Al_2O_3 of 3.83 according to the highest compressive strength at the age of 28 days and high fly ash content. The optimal mixture was 27.0, 32.4, and 25.6%, with the ratio SiO_2/Al_2O_3 of 4.01 in case of highest compressive strength at 56 days, respectively. As a result, compressive strength tends to rise with increased GGBS content of about 25% at a later age of 28 days.

- The compressive strength of mortar specimen using the firstly optimal AAC up to 28 days was lower than that in the case of PC40 cement but about 16% higher at 56 days.

5. Declarations

5.1. Data Availability Statement

The data presented in this study are available in article.

5.2. Funding

5.3. Acknowledgements

5.4. Conflicts of Interest

The author declares no conflict of interest.

6. References

[1] Caijun Shi, Della Roy, and Pavel Krivenko. "Alkali-Activated Cements and Concretes" (May 10, 2006), Taylor & Francis.

[2] Grant Norton, M., Provis, J.L. "1000 at 1000: Geopolymer technology- the current state of the art." Journal of Materials Science 55 (October 2020): 13487–13489. doi.org/10.1007/s10853-020-04990-z.

[3] F. Pacheco-Torgal, J. Castro-Gomes, and S. Jalali. "Alkali-activated binders: A review: Part 1. Historical background, terminology, reaction mechanisms, and hydration products." Construction and Building Materials 22 (July 2008): 1305-1314, doi.org/10.1016/j.conbuildmat.2007.10.015.

[4] Palomo, P. Krivenko, I. García-Lodeiro, E. Kavalerova, O. Maltseva, and A. Fernández-Jiménez, "A review on alkaline activation: New analytical perspectives," Materiales de Construccion 64 (July-September 2014): 1-24, doi.org/10.3989/mc.2014.00314.

[5] Krivenko, Pavel, Oleksandr Kovalchuk, Anton Pasko, Tom Croymans, Mikael Hult, Guillaume Lutter, Niels Vandevenne, Sonja Schreurs, and Wouter Schroeyers. "Development of Alkali Activated Cements and Concrete Mixture Design with High Volumes of Red Mud." Construction and Building Materials 151 (October 2017): 819–826. doi:10.1016/j.conbuildmat.2017.06.031.

[6] Davidovits, Joseph. "Environmentally driven geopolymer cement applications." In Proceedings of 2002 Geopolymer Conference. Melbourne. Australia. 2002.

[7] Jiang, Mohan, Xiaoju Chen, Farshad Rajabipour, and Chris T. Hendrickson. "Comparative Life Cycle Assessment of Conventional, Glass Powder, and Alkali-Activated Slag Concrete and Mortar." Journal of Infrastructure Systems 20, no. 4 (December 2014): 04014020. doi:10.1061/(asce)is.1943-555x.0000211.

[8] Bach, D T, V L Hoang, and N B Nguyen. "Pelletized Fly Ash Aggregates Use for Making Eco-Friendly Concrete." IOP Conference Series: Materials Science and Engineering 869 (July 10, 2020): 032028. doi:10.1088/1757-899x/869/3/032028.

[9] Food and Agriculture Organization (FAO), FAOSTAT, 2019. Available online: http://www.fao.org/faostat/en/#data/QC. (accessed on March 2021).

[10] Abbas, Anwar Saad, and Mohammed Mansour Kadhum. "Impact of Fire on Mechanical Properties of Slurry Infiltrated Fiber Concrete (SIFCON)." Civil Engineering Journal 6 (September 30, 2020): 12–23. doi:10.28991/cej-2020-sp(emce)-02.

[11] "Using granulated blast furnace slag: Reduce CO_2 emissions, improve construction quality." Newspaper of Resources and Environment (in Vietnamese: "Sử dụng xỉ hạt lò cao: Giảm phát thải CO_2, nâng cao chất lượng công trình xây dựng." Báo Tài nguyên và Môi trường). Available online: https://baotainguyenmoitruong.vn/su-dung-xi-hat-lo-cao-giam-phat-thai-co2-nang-cao-chat-luong-cong-trinh-xay-dung-239325.html (accessed on February 2021).

[12] Nath, Pradip, and Prabir Kumar Sarker. "Effect of GGBFS on Setting, Workability and Early Strength Properties of Fly Ash Geopolymer Concrete Cured in Ambient Condition." Construction and Building Materials 66 (September 2014): 163–171. doi:10.1016/j.conbuildmat.2014.05.080.

[13] Songpiriyakij, Smith, Tawich Pulngern, Pompong Pungpremtrakul, and Chai Jaturapitakkul. "Anchorage of Steel Bars in Concrete by Geopolymer Paste." Materials & Design 32, no. 5 (May 2011): 3021–3028. doi:10.1016/j.matdes.2011.01.048.

[14] Matalkah, Faris, and Parviz Soroushian. "Synthesis and Characterization of Alkali Aluminosilicate Hydraulic Cement That Meets Standard Requirements for General Use." Construction and Building Materials 158 (January 2018): 42–49. doi:10.1016/j.conbuildmat.2017.10.002.

[15] Darsanasiri, A.G.N.D., Faris Matalkah, Salina Ramli, Kutaibah Al-Jalode, Anagi Balachandra, and Parviz Soroushian. "Ternary Alkali Aluminosilicate Cement Based on Rice Husk Ash, Slag and Coal Fly Ash." Journal of Building Engineering 19 (September 2018): 36–41. doi:10.1016/j.jobe.2018.04.020.

[16] Mejía de Gutiérrez, R., J. M. Mejía, and F. Puertas. "Ceniza de Cascarilla de Arroz Como Fuente de Sílice En Sistemas Cementicios de Ceniza Volante y Escoria Activados Alcalinamente." Materiales de Construcción 63, no. 311 (September 20, 2013): 361–375. doi:10.3989/mc.2013.04712.

[17] Bernal, Susan A., Erich D. Rodríguez, Ruby Mejia de Gutiérrez, John L. Provis, and Silvio Delvasto. "Activation of Metakaolin/Slag Blends Using Alkaline Solutions Based on Chemically Modified Silica Fume and Rice Husk Ash." Waste and Biomass Valorization 3, no. 1 (October 7, 2011): 99–108. doi:10.1007/s12649-011-9093-3.

[18] Provis, John L., Peter Duxson, Grant C. Lukey, and Jannie S. J. van Deventer. "Statistical Thermodynamic Model for Si/Al Ordering in Amorphous Aluminosilicates." Chemistry of Materials 17, no. 11 (May 2005): 2976–2986. doi:10.1021/cm050219i..

[19] Diaz, E.I., E.N. Allouche, and S. Eklund. "Factors Affecting the Suitability of Fly Ash as Source Material for Geopolymers." Fuel 89, no. 5 (May 2010): 992–996. doi:10.1016/j.fuel.2009.09.012.

[20] Rashad, Alaa M. "A Comprehensive Overview About the Influence of Different Admixtures and Additives on the Properties of Alkali-Activated Fly Ash." Materials & Design 53 (January 2014): 1005–1025. doi:10.1016/j.matdes.2013.07.074.

[21] He, Pingping, Binyu Zhang, Jian-Xin Lu, and Chi Sun Poon. "A Ternary Optimization of Alkali-Activated Cement Mortars Incorporating Glass Powder, Slag and Calcium Aluminate Cement." Construction and Building Materials 240 (April 2020): 117983. doi:10.1016/j.conbuildmat.2019.117983.

[22] Venkatesan, Mayandi, Qammer Zaib, Izhar Hussain Shah, and Hung Suck Park. "Optimum Utilization of Waste Foundry Sand and Fly Ash for Geopolymer Concrete Synthesis Using D-Optimal Mixture Design of Experiments." Resources, Conservation and Recycling 148 (September 2019): 114–123. doi:10.1016/j.resconrec.2019.05.008.

[23] ASTM C150/C150M-20, Standard Specification for Portland Cement, ASTM International, West Conshohocken, PA, (2020).

[24] ISO 9597:2008 Cement - Test methods - Determination of setting time and soundness (2008).

[25] ISO 679:2009 Cement - Test methods - Determination of strength (2009).

[26] Chindaprasirt, Prinya, Pre De Silva, Kwesi Sagoe-Crentsil, and Sakonwan Hanjitsuwan. "Effect of SiO_2 and Al_2O_3 on the Setting and Hardening of High Calcium Fly Ash-Based Geopolymer Systems." Journal of Materials Science 47, no. 12 (March 3, 2012): 4876–4883. doi:10.1007/s10853-012-6353-y.

[27] Palomo, A., M.W. Grutzeck, and M.T. Blanco. "Alkali-Activated Fly Ashes." Cement and Concrete Research 29, no. 8 (August 1999): 1323–1329. doi:10.1016/s0008-8846(98)00243-9.

[28] L.T. Thành and N. C. Thắng. "Influence of ground granulated blast-furnace slag on the viscosity of binder paste for production of UHPC." Tạp chí Khoa học Công nghệ Xây dựng 11 (2017): 16-21.

[29] Vietnam Standard TCVN 2682: 2009. "Portland cement – Specifications.", (2009).

[30] Thắng, N. C., Thắng, N. T., Hanh, P. H., Tuấn, N. V., and Lâm, N. T. "Ultra high performance concrete using a combination of Silica Fume and ground granulated blast-furnace slag in Vietnam," Tạp chí Khoa học Công nghệ Xây dựng, 7 (2013):83-92.